ARCHIVES OF ELECTRICAL ENGINEERING VOL. 67(4), pp. 885–898 (2018)

DOI 10.24425/aee.2018.124747

Improved dynamic control method for energy storage units in PV dominated microgrids

QINGBO WANG[1], YIQI LIU[1], WENLONG SONG[1], KE XUAN[2]

[1] *Northeast Forestry University*
26 Hexing Road, Xiangfang District, Harbin, China
e-mail: ee_617@nefu.edu.cn

[2] *State Grid Company, Heilongjiang Branch*
85 Wenjing street, Xiangfang District, Harbin, China

(Received: 24.06.2018, revised: 11.09.2018)

Abstract: In a PV-dominant DC microgrid, the traditional energy distribution method based on the droop control method has problems such as output voltage drop, insufficient power distribution accuracy, etc. Meanwhile, different battery energy storage units usually have different parameters when the system is running. Therefore, this paper proposes an improved control method that introduces a reference current correction factor, and a weighted calculation method for load power distribution based on the parameters of battery energy storage units is proposed to achieve weighted allocation of load power. In addition, considering the variation of bus voltage at the time of load mutation, voltage secondary control is added to realize dynamic adjustment of DC bus voltage fluctuation. The proposed method can achieve balance and stable operation of energy storage units. The simulation results verified the effectiveness and stability of the proposed control strategy.

Key words: current correction coefficient, load distribution, PV DC microgrid, secondary control, weighted calculation

1. Introduction

Compared to traditional AC microgrids, DC microgrids feature higher stability without considering reactive power, frequency, and phase. Since no reactive power flow exists in the system, the voltage becomes the only indicator of the power balance of the DC microgrid system [1, 2]. Meanwhile, with the increase of new energy devices, which use DC power as their energy sources, the energy conversion process from AC/DC to DC/DC in AC microgrids not only increases the complexity of the system but also makes it difficult to control. The loss in the transformation process also involves energy waste, so DC microgrids have received more and more attention [3]. In a DC microgrid, photovoltaic power generation has become a research hotspot at home and abroad because of its clean and flexible installation. In PV-dominated DC microgrids, due to

the intermittent and fluctuation of PV generation, it is necessary to use a connection method combined with energy storage to realize the system energy supply.

Considering the load power demand and guaranteeing the safe and stable system operation, a number of energy storage units are generally used in PV DC microgrids. Since the differences of parameters such as the state-of-charge (SOC), capacity and maximum input/output power of the battery storage units during system operation, the load power distribution should also be different. The common load distribution methods include centralized control [4] and decentralized control [5, 6]. In the decentralized control, the droop control is dominant. However, although the droop control structure is simple, there are problems such as insufficient power distribution accuracy and output voltage drop [6, 8, 9]. For centralized control, although there are higher communication requirements, with the maturity of related technologies, the superiority of using centralized control is gradually emerging.

In [7], an improved droop control strategy is proposed. However, droop control will cause a certain degree of voltage drop, the solution to this problem is not mentioned in the paper. In order to solve the problem of droop control accuracy, an active identification method for line resistance is proposed in [8]. In [9], a droop control method is proposed to solve the problem of current distribution accuracy and voltage deviation in traditional droop control. A modified strategy for load power sharing accuracy enhancement in a droop-controlled DC microgrid is proposed in [10]. A hybrid energy storage control method of the DC microgrid is proposed [11]. However, the cost of the super-capacitor is relatively high for a DC microgrid that utilizes super-capacitors as energy storage. Meanwhile, super-capacitors only play a role when disturbance occurs. In [12], an accurate power sharing method to balance the state of charge (SOC) among the distributed battery energy units (BEUs) in a DC microgrid is proposed. In [13], a load power distribution method based on the state of charge (SOC) of the battery energy storage unit is proposed. However, regarding the distribution of load power, only the discharging process is considered, and the control of the charging process is not mentioned.

This paper takes the PV-dominated DC microgrids as the research object.

1. Aiming at the problems of voltage drop and low power distribution accuracy caused by the defects of a traditional droop control method, the control method of current correction coefficient is proposed. This method does not have the problem of voltage drop and degraded control accuracy, and improves system stability.
2. Considering, that the control method of energy storage in the existing literature does not take into account the effects of various parameters of energy storage unit. In this paper, a weighted calculation method of load power distribution based on battery SOC, capacity and maximum input (output) power is proposed, and the accurate distribution of load power can be further realized.
3. For problems such as low utilization rate and poor economic efficiency of hybrid energy storage control methods adopted in some control methods. In this paper, the secondary voltage regulation method can automatically adjust the bus voltage value according to the fluctuation of voltage, and automatically 'fail' in stable operation, realizing the dynamic elimination of bus voltage fluctuation.

The effectiveness of the proposed strategy is verified based on the MATLAB/Simulink simulation results.

2. Load distribution calculation in PV-dominated DC microgrids

A PV-dominated DC microgrid system structure shown in Fig. 1:

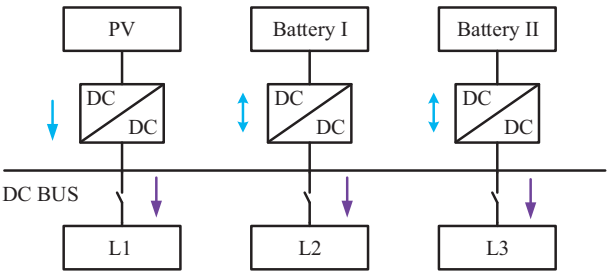

Fig. 1. PV DC microgrid system structure

PV DC microgrids include photovoltaic power generation units, energy storage units, energy converters, and loads. The PV generation unit is generally operated in a maximum power point tracking (MPPT) mode, and a boost converter is used to connect the DC bus. The energy storage unit uses a DC-DC bidirectional converter to connect the DC bus. When the system runs steadily, the following equation is established [14]:

$$P_L - P_V = P_B, \tag{1}$$

where P_L represents the total power of the load in the DC microgrid, P_V represents the total output power of the photovoltaic power generation unit, and P_B represents the total output power of all energy storage units.

Microgrid can adopt different operation strategies, such as operation strategy based on preset fixed logic rules and operation strategy based on economic dispatch. When priority is given to using microgrid internal renewable energy to generate electricity, the following operation strategies can be used:

1. When the PV output is greater than the load demand, the excess power is preferentially charged to the battery, and the remaining power that the battery cannot absorb is sent to the grid (if permitted),
2. When the PV output cannot meet the load demand, in order to reduce the purchase of electricity from an external grid, the battery is preferentially discharged, and the SOC state of the battery is detected,
3. When the total output power of the PV and battery cannot meet the load demand, then the power is purchased from the grid to meet the load demand.

The load distribution method described herein is based on a stable operating environment in which photovoltaic power is directly supplied to the load and stored energy. Deeper microgrid economic dispatch is beyond the scope of this article.

In this paper, the PV-dominated DC microgrid containing two energy storage units is taken as an example, and a weighted calculation method for load power distribution based on the parameters of the battery energy storage unit is proposed. According to the impact degree of each parameter on the output power distribution of the battery to rationally assign their weight coefficient, the

battery's three parameters are used for weighted calculation. These three parameters are SOC of the battery, the maximum output power of the energy storage unit, and battery storage capacity. The specific calculation method is as follows:

$$P_1 = \frac{P_{M1}}{P_{M1} + P_{M2}}, \qquad P_2 = \frac{P_{M2}}{P_{M1} + P_{M2}}. \tag{2}$$

In Equation (2), P_{M1} and P_{M2} are the maximum input (output) power of energy storage units I and II, respectively, and P_1 and P_2 are the proportions of energy storage units I and II in the total maximum input (output) power of the energy storage system.

$$s_1 = \frac{\mathrm{SOC}_1}{\mathrm{SOC}_1 + \mathrm{SOC}_2}, \qquad s_1' = \frac{100 - \mathrm{SOC}_1}{(100 - \mathrm{SOC}_1) + (100 - \mathrm{SOC}_2)}, \tag{3}$$

$$s_2 = \frac{\mathrm{SOC}_2}{\mathrm{SOC}_1 + \mathrm{SOC}_2}, \qquad s_2' = \frac{100 - \mathrm{SOC}_2}{(100 - \mathrm{SOC}_1) + (100 - \mathrm{SOC}_2)}. \tag{4}$$

In Equation (3) and Equation (4), SOC_1 and SOC_2 are the SOC of energy storage units I and II, respectively. s_1 and s_2 are the proportions of energy storage units I and II in the total SOC of an energy storage system during the discharging process, $s_1^{'}$ and $s_2^{'}$ are the proportions of energy storage units I and II in the total counting SOC of the energy storage system during the charging process.

$$a_1 = \frac{A_1}{A_1 + A_2}, \qquad a_2 = \frac{A_2}{A_1 + A_2}. \tag{5}$$

In Equation (5), A_1 and A_2 are the battery capacities of energy storage units I and II, respectively. a_1 and a_2 are the proportions of energy storage units I and II in the total counting capacity of the energy storage system.

$$A_{b1} = k_p P_1 + k_s s_1 + k_a a_1, \qquad A_{b1}' = k_p P_1 + k_s s_1' + k_a(1 - a_1), \tag{6}$$

$$A_{b2} = k_p P_2 + k_s s_2 + k_a a_2, \qquad A_{b2}' = k_p P_2 + k_s s_2' + k_a(1 - a_2). \tag{7}$$

In Equation (6) and Equation (7), k_p, k_s and k_a represent respectively the weights assigned by the three parameters of the maximum output power of the energy storage unit, the SOC and the capacity of the battery storage unit according to their influence on the battery load power distribution. A_{b1} and A_{b2} respectively represent the load power distribution parameters calculated according to the parameters of energy storage units I and II during discharging process, A_{b1}' and A_{b2}' represent the load power distribution parameters calculated according to the parameters of energy storage units I and II respectively during charging process. Since the charge and discharge capacity of the battery is determined by its maximum output power. Therefore, a uniform setting is used for this parameter during the charging and discharging process.

For the selection of k_p, k_s, and k_a. Since the main goal is to reasonably allocate the output power of the battery storage unit and prevent the over-charge and over-discharge of the battery unit, k_s is relatively large. Since in the same DC microgrid, the battery capacity among different energy storage units is substantially the same, k_a is relatively small. The relationship between the size of the three weights is $k_s > k_p > k_a$.

The calculation method of the reference value of the load distribution power of energy storage unit I is as follows, and the calculation method of energy storage unit II is the same.

The distribution power for energy storage unit I during discharging is as follows:

$$P_{B1} = \frac{A_{b1}}{A_{b1} + A_{b2}} P_B \,. \tag{8}$$

The distribution power during the charging process is as follows:

$$P'_{B1} = \frac{A'_{b1}}{A'_{b1} + A'_{b2}} P_B \,. \tag{9}$$

The switching of the charging and discharging process control method can be realized by judging the direction of the inductor current in the bidirectional voltage converter of the battery in the energy storage unit.

The load power distribution method proposed in this paper is based on the traditional double-loop control method, which is achieved by dynamically adjusting the reference value of inductor current of bi-directional energy storage converter in the inner current loop. The specific structure is shown in Fig. 2:

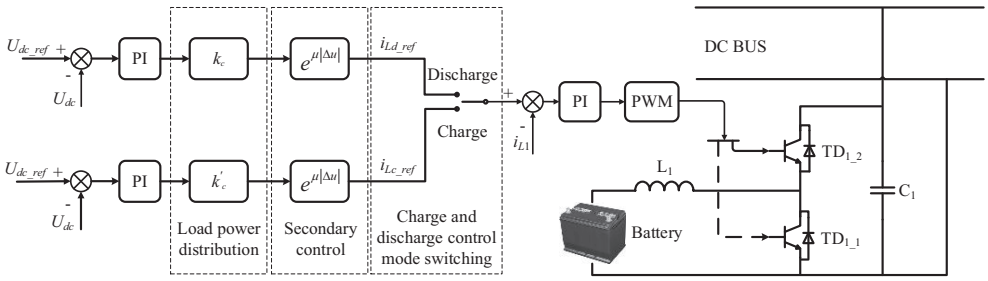

Fig. 2. Energy storage unit and its control structure

Here is an example of the discharging process of energy storage unit I.

For the load power distribution link, the calculation of control parameters is based on the load distribution powers of Equations (8) and (9). The expression is:

$$k_c = k_{iL} \frac{P_{B1}}{P_{B1} + P_{B2}}, \tag{10}$$

where k_{iL} is the parameter related to the inductor current correction coefficient, and the value here is 2. This can make the sum of the reference current correction coefficients of two energy storage batteries equal 2.

3. Reference current secondary control based on the voltage deviation

Considering the situation that when the load changes, the power balance in the DC microgrid is violated and eventually the bus voltage changes. When the voltage change is too large, it will lead to a fault for the system. In this paper, a secondary control method based on bus voltage deviation is proposed to realize the secondary dynamic adjustment of the reference current according to

the bus voltage when the bus voltage deviation is large. The specific control method is shown in Fig. 2, in which the structural expression of the secondary link is:

$$k_s = e^{\mu|\Delta u|}, \tag{11}$$

where Δu is the deviation between the actual value of the bus voltage and the reference value, and μ is a parameter related to the degree of influence of the voltage fluctuation on the reference current. The value of μ in different energy storage units is determined by the reference load distribution power of the different energy storage units calculated above, and there are positive and negative differences. Its positive and negative values are selected as shown in Fig. 3:

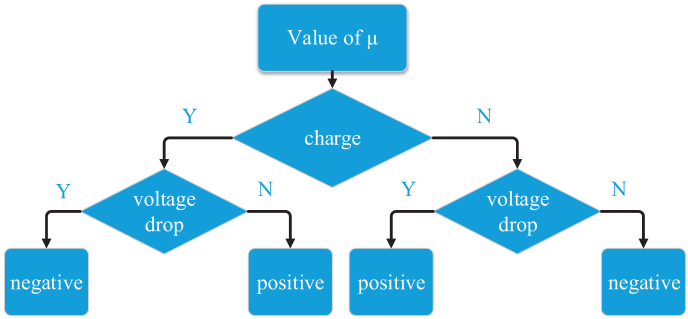

Fig. 3. The value judgment flow chart of μ

Specific conditions are as follows:

1. If the bus voltage drops momentarily after the disturbance occurs and the battery unit is operating in the charging state during the disturbance, then the value of μ should be negative.
2. If the bus voltage drops momentarily after the disturbance occurs and the battery unit is operating in the discharge state during the disturbance, the value of μ should be positive.
3. If the bus voltage rises momentarily after the disturbance occurs and the battery unit is operating in the charge state during the disturbance, the value of μ should be positive.
4. If the bus voltage rises momentarily after the disturbance occurs and the battery unit is operating in the discharge state during the disturbance, the value of μ should be negative at this time.

Since the value of μ is relatively small, it can be seen from Equation (11) that the value of Equation (11) is 1 when the system is operating stably. That is, the secondary dynamic adjustment of the reference current during steady operation does not affect the power distribution. When the bus voltage fluctuates, the current control parameters are dynamically adjusted according to the voltage fluctuations to achieve a stable system.

4. Stability analysis

For the secondary control of the system, since the value of μ is very small, the secondary control link can be equivalent to:

$$e^{\mu\Delta u} \approx 1 + k_\mu \Delta u. \tag{12}$$

Therefore, the system small signal model is shown in Fig. 4 can be obtained.

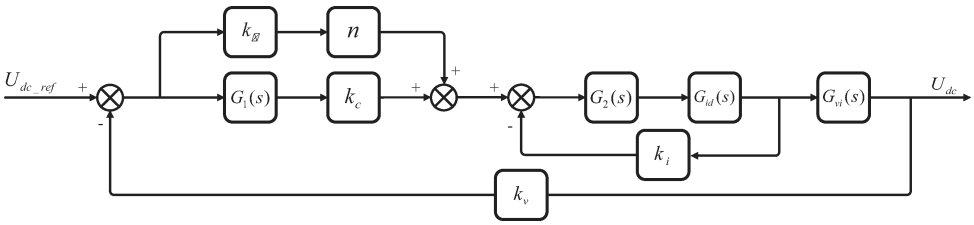

Fig. 4. System small-signal model

In Fig. 4, k_c represents the current correction coefficient calculated at the load power distribution section, and n represents the stable output from this section. $G_1(s)$, $G_2(s)$ are the transfer functions of the voltage loop and the current loop, respectively. $G_{id}(s)$, $G_{vi}(s)$ are the transfer functions of the converter duty ratio d to the inductor current i_L, the inductor current i_L to the output voltage U_{dc}, respectively [15]. k_i and k_v are the feedback coefficients of i_L and U_{dc}, respectively, and the values here all equal 1. From this the open-loop small-signal transfer function of the system can be derived:

$$G_k(s) = \left(G_1(s)k_c + k_\mu n\right) \frac{G_2(s)G_{id}(s)G_{vi}(s)}{1 + G_2(s)G_{id}(s)} . \tag{13}$$

In the formula:

$$G_1(s) = k_{p1} + k_{i1}/s, \tag{14}$$

$$G_2(s) = k_{p2} + k_{i2}/s. \tag{15}$$

Bringing in the system parameters can give a Bode plot of an open-loop system as shown in Fig. 5. It can be seen from the figure that the phase margin of the system is $\gamma > 90°$, so it can be considered that the system is stable.

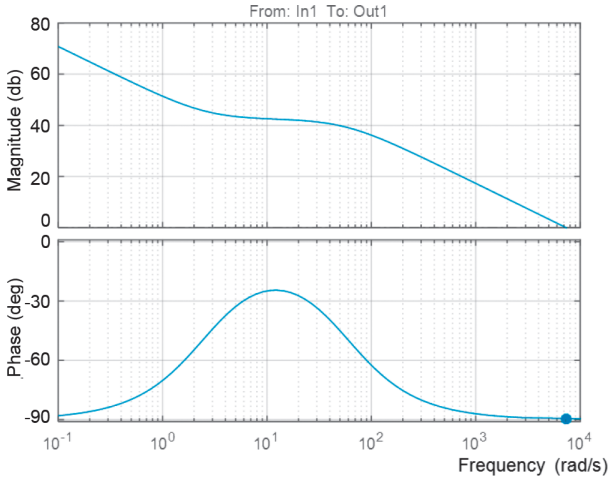

Fig. 5. Bode diagram of the open loop system

5. Simulation results

In order to verify the effectiveness of the proposed control strategy, a PV-dominated DC microgrid system as shown in Fig. 1 is built in Simulink.

Its basic operating condition is:

1. The maximum output power of the photovoltaic power generation unit is 10 kW, and it works in MPPT mode.
2. Energy storage unit I selects a battery with a maximum output of 10 kW, a capacity of 2 Ah and an initial SOC of 80%. Energy storage unit II selects a battery with a maximum output of 5 kW, a capacity of 2 Ah, and an initial SOC of 50%. Meanwhile, the SOC of energy storage unit I and energy storage unit II are kept at 10%-90% during operation.
3. The initial load of the DC microgrid system is L_1 with a resistance of 25 Ω, load L_2 with a resistance of 50 Ω is added at 0.5 s, and load L_3 with a resistance of 100 Ω is added at 1 s. The simulation time is 1.5 s, for k_p, k_s and k_a from the above analysis, here are set to 0.3, 0.5, and 0.2, respectively.

The simulation experiment results are run in the following three work conditions:

1. The control method of the energy storage unit in operating condition I is the traditional double-loop control (voltage outer loop, current inner loop).
2. The control method of the energy storage unit in operating condition II is a double-loop control including a current correction coefficient control link.
3. The control method of the energy storage unit in condition III includes the current correction coefficient control and the reference current secondary control.

The specific simulation results are as follows:

Fig. 6 shows the bus voltage curve of the DC microgrid.

The data in Fig. 6 shown in Table 1.

Table 1. Bus voltage variation under different operating conditions

Operating condition	First disturbance	Second disturbance
Condition I	4.8 V	2.6 V
Condition II	4.8 V	2.5 V
Condition III	2.9 V	1.9 V

It can be seen from Table 1 that the bus voltage changes in operating condition II is almost the same as the change of bus voltage in operating condition I. Compared to operating conditions III and II, the voltage fluctuation amplitude is significantly reduced.

Fig. 7 shows the SOC curve of energy storage units I and II under different operating conditions.

The data from Fig. 7 is shown in Table 2.

From the above data, it can be seen that the SOC variation of energy storage units I and II is almost the same in condition I. In the charging process of operating condition II and operating condition III, the variation of SOC of energy storage unit I is smaller than the variation of SOC of energy storage unit II. The variation of SOC of energy storage unit I during discharging is greater than the variation of SOC of energy storage unit II.

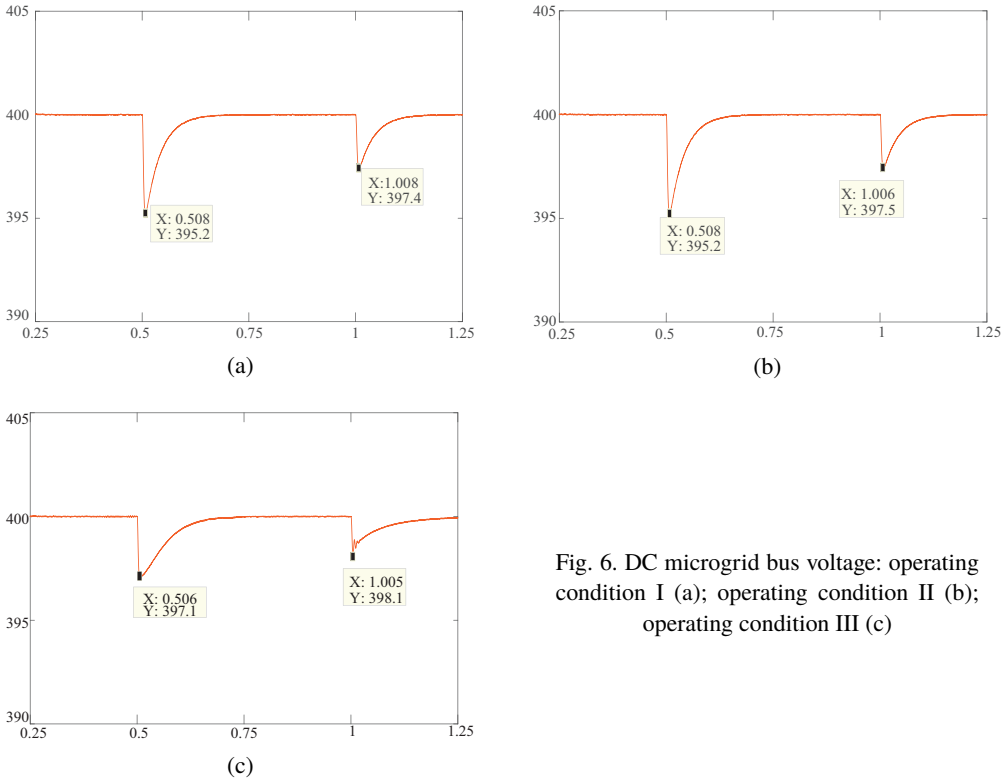

Fig. 6. DC microgrid bus voltage: operating condition I (a); operating condition II (b); operating condition III (c)

Table 2. The SOC variation under different conditions

Operating condition	Period	Storage unit I	Storage unit II	Ratio
Condition I	0 s ~ 0.5 s	0.10673%	0.10579%	1.0089
	0.5 s ~ 1 s	0.00908%	0.00866%	1.0485
	1 s ~ 1.5 s	−0.0454%	−0.04531%	1.020
Condition II	0 s ~ 0.5 s	0.09359%	0.11813%	0.7923
	0.5 s ~ 1 s	0.00841%	0.01015%	0.8285
	1 s ~ 1.5 s	−0.05563%	−0.03473%	1.6017
Condition III	0 s ~ 0.5 s	0.09435%	0.11859%	0.7956
	0.5 s ~ 1 s	0.00835%	0.00968%	0.8626
	1 s ~ 1.5 s	−0.05564%	−0.03517%	1.5820

Fig. 8 shows the input/output power curves of energy storage units I and II.

The data in Fig. 8 shown in Table 3.

From the above data, it can be seen that the data are in accordance with the variation of the SOC.

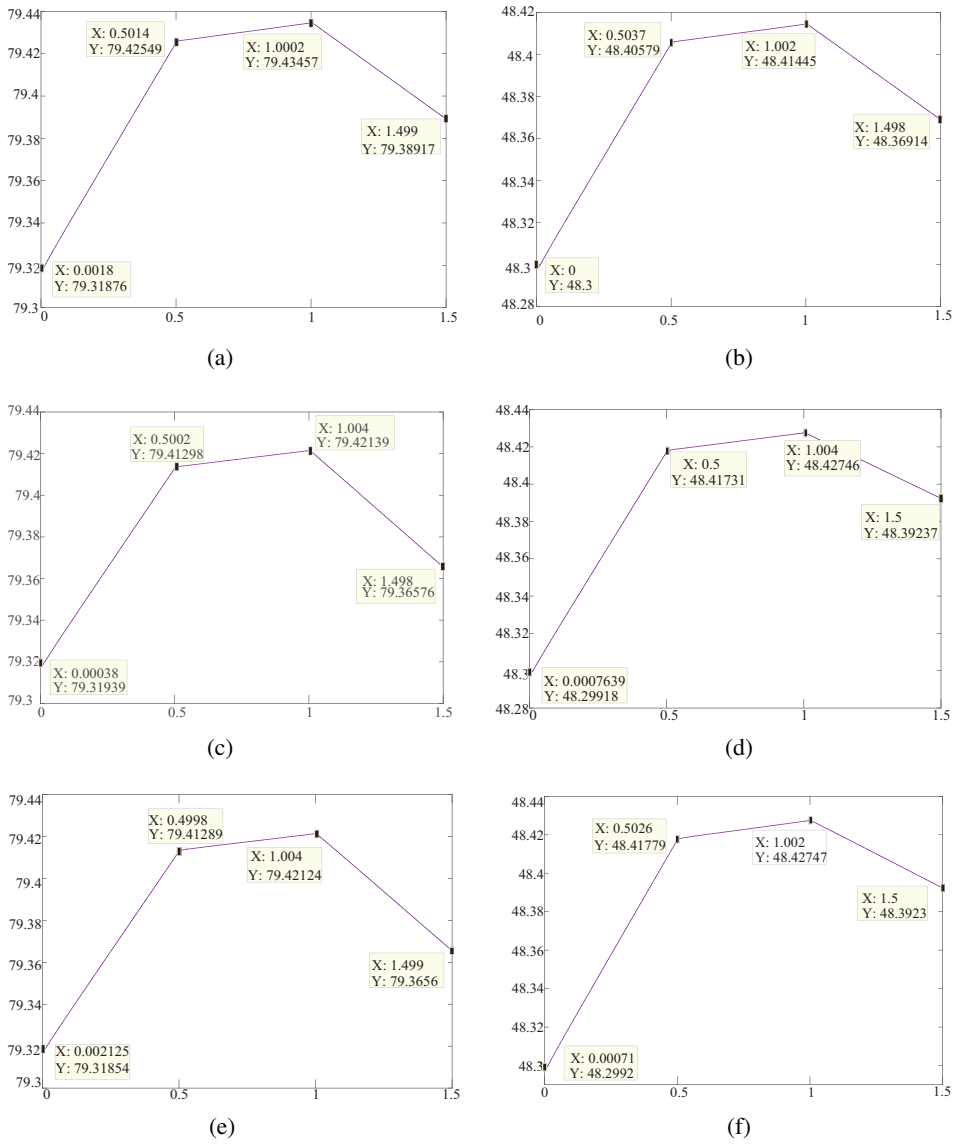

Fig. 7. SOC of energy storage unit I and II in different conditions: unit I in condition I (a); unit II in condition I (b); unit I in condition II (c); unit II in condition II (d); unit I in condition III (e); unit II in condition III (f)

The following example illustrates the role of the secondary control.

Fig. 9 shows the power change of energy storage unit I in operating conditions II and III:

The curves $Pbat1_3$ and $Pbat1_2$ in Fig. 9 respectively represent the power variation curves of energy storage unit I in operating conditions III and II. It can be seen from the figures that during a period of time after 0.5 s, the charge power of energy storage unit I in condition III is significantly

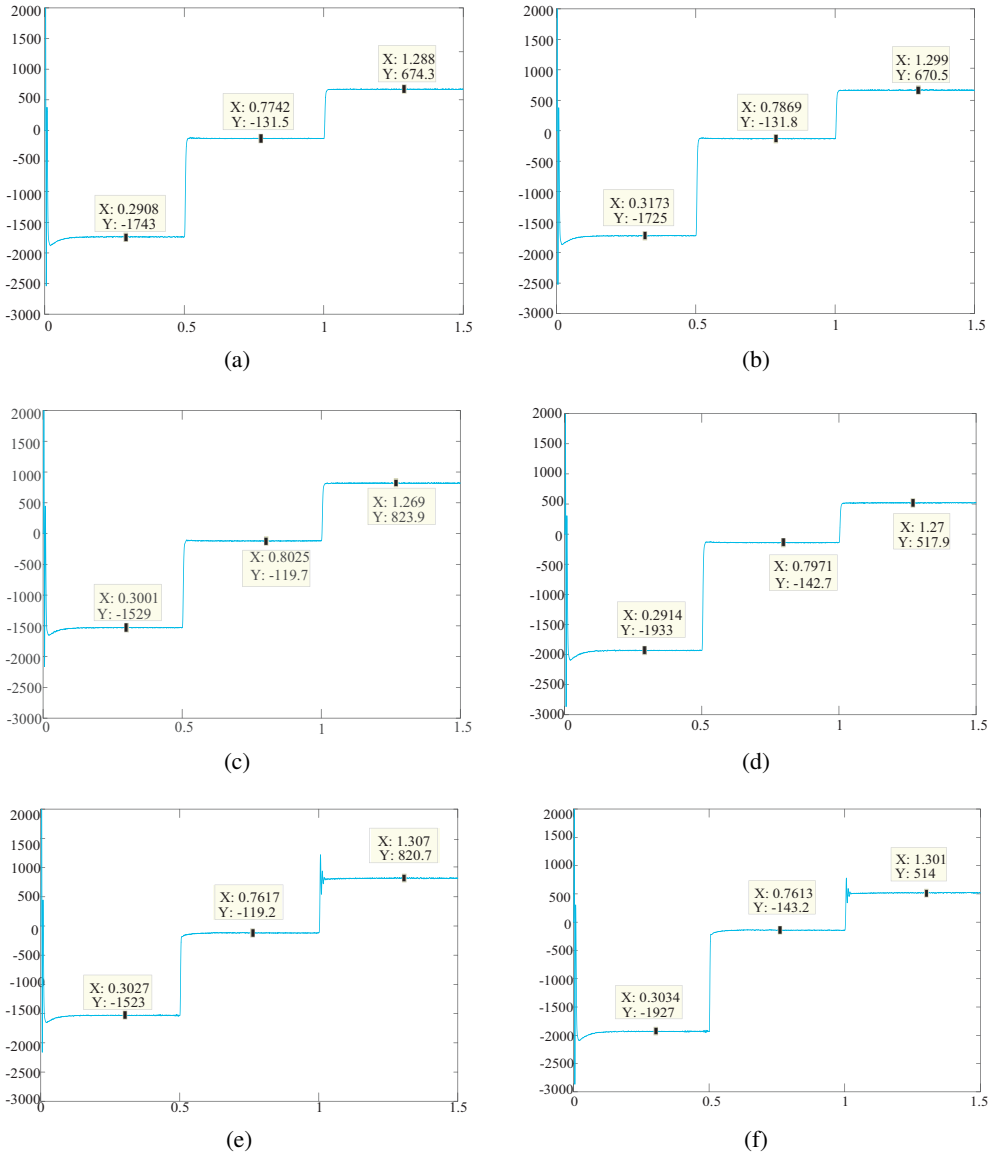

Fig. 8. Input/output power curves of energy storage units I and II in different operating conditions: unit I in condition I (a); unit II in condition I (b); unit I in condition II (c); unit II in condition II (d); unit I in condition III (e); unit II in condition III (f)

less than the charge power in condition II. During a period of time after 1 s, the discharge power of energy storage unit I in operating condition III is obviously greater than the discharge power in operating condition II. These two conditions correspond to the value of μ above. The system introducing the secondary control can automatically change the charging and discharging power

Table 3. Power variation under different operating conditions

Operating condition	Period	Storage unit I	Storage unit II
Condition I	0 s ~ 0.5 s	1.7 kW	1.7 kW
	0.5 s ~1 s	0.13 kW	0.13 kW
	1 s ~ 1.5 s	0.67 kW	0.67 kW
Condition II	0 s ~ 0.5 s	1.5 kW	1.9 kW
	0.5 s ~ 1 s	0.12 kW	0.14 kW
	1 s ~ 1.5 s	0.8 kW	0.5 kW
Condition III	0 s ~ 0. s	1.5 kW	1.9 kW
	0.5 s ~ 1 s	0.12 kW	0.14 kW
	1 s ~ 1.5 s	0.8 kW	0.5 kW

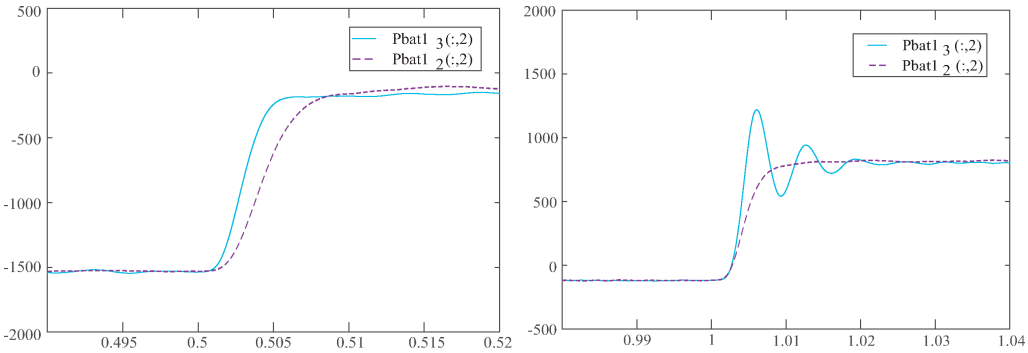

(a) (b)

Fig. 9. Power variation of energy storage unit I in operating conditions II and III: after 0.5 s (a); after 1.0 s (b)

according to the voltage deviation during the charging and discharging process. In addition, it can be seen in the figure that the power change of energy storage unit I in operating conditions II and III is almost the same when the system tends to operate stably. It shows that the secondary control introduced will not affect the system when the system is stable, and it is in line with the analysis above, and it has achieved the effect of the automatic adjustment.

Fig. 10 shows the current correction coefficient.

It can be seen from the data in the Fig. 10 that the ratio of the correction coefficients of the two controllers is 0.8 before 1 s, and the ratio after 1 s is about 1.6. Compared to the data of Fig. 7 and Fig. 8, it can be seen that the change of the correction coefficient corresponds to the change of the SOC and the charge and discharge power of the energy storage unit in the system. It is shown that the proposed method can realize automatic switching of control parameters in the charge and discharge process, so that the system can realize reasonable distribution of load power.

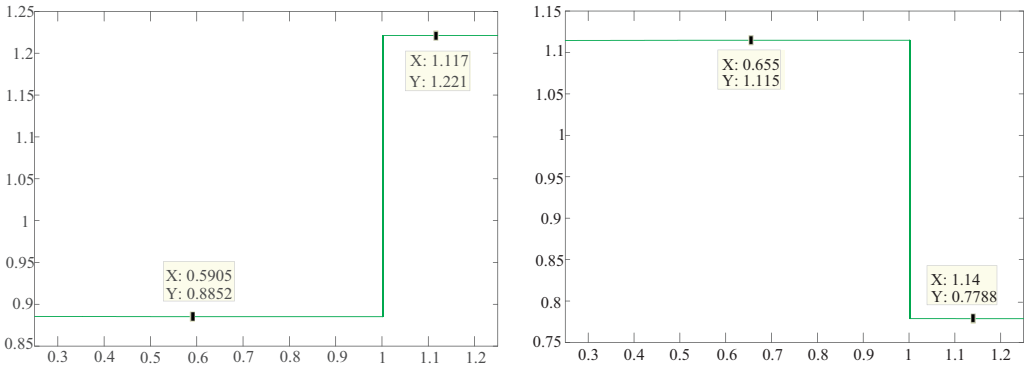

(a) (b)

Fig. 10. Current correction coefficients of energy storage unit I and II: unit I (a); unit II (b)

6. Conclusions

This paper proposes an improved dynamic load distribution method for PV-dominated DC microgrids. With simulation analysis, the following conclusions are listed as follows:

1. After the secondary control is activated, the amplitude of bus voltage fluctuation is significantly reduced.
2. Compared to traditional control method, the improved control method presented in this paper does not adversely affect the bus voltage and power of the original system.
3. The control method proposed in this paper can achieve a reasonable distribution of load power, and it can automatically adjust the control parameters according to the switching of charging and discharging process.

Acknowledgements

This work was supported by China Postdoctoral Science Foundation funded project (No. 2018M631893) and Harbin Municipal Science and Technology Bureau Innovative Talent Foundation (No. 2017RAQXJ044).

References

[1] Liu L., Mi Z., Ren C., Qin W., Han X., Wang P., *Coordination control strategy of DC microgrid with two DC buses based on power pool*, 2017 12th IEEE Conference on Industrial Electronics and Applications (ICIEA), Siem Reap, KHM, pp. 1437–1442 (2017).

[2] Zhang L., Wang Y., Li H., Sun P., *Hierarchical coordinated control of DC microgrid with wind turbines*, IECON 2012 – 38th Annual Conference on IEEE Industrial Electronics Society, Montreal, QC, pp. 3547–3552 (2012).

[3] Anand S., Fernandes B.G., Guerrero J., *Distributed Control to Ensure Proportional Load Sharing and Improve Voltage Regulation in Low-Voltage DC Microgrids*, IEEE Transactions on Power Electronics, vol. 28, no. 4, pp. 1900–1913 (2013).

[4] Tsikalakis A.G., Hatziargyriou N.D., *Centralized Control for Optimizing Microgrids Operation*, IEEE Transactions on Energy Conversion, vol. 23, no. 1, pp. 241–248 (2008).

[5] Anand S., Fernandes B.G., *Modified droop controller for paralleling of dc-dc converters in standalone dc system*, IET Power Electronics, vol. 5, no. 6, pp. 782–789 (2012).

[6] Augustine S., Mishra M.K., Lakshminarasamma N., *Adaptive Droop Control Strategy for Load Sharing and Circulating Current Minimization in Low-Voltage Standalone DC Microgrid*, IEEE Transactions on Sustainable Energy, vol. 6, no. 1, pp. 132–141 (2015).

[7] Hu R., Weaver W.W., *Dc microgrid droop control based on battery state of charge balancing*, 2016 IEEE Power and Energy Conference at Illinois (PECI), Urbana, IL, pp. 1–8 (2016).

[8] Liu C., Zhao J., Wang S., Lu W., Qu K., *Active Identification Method for Line Resistance in DC Microgrid Based on Single Pulse Injection*, IEEE Transactions on Power Electronics, vol. 33, no. 7, pp. 5561–5564 (2018).

[9] Lu X., Guerrero J.M., Sun K., Vasquez J.C., *An Improved Droop Control Method for DC Microgrids Based on Low Bandwidth Communication with DC Bus Voltage Restoration and Enhanced Current Sharing Accuracy*, IEEE Transactions on Power Electronics, vol. 29, no. 4, pp. 1800–1812 (2014).

[10] Liu Y., Wang J., Li N., Fu Y., Ji Y., *Enhanced load power sharing accuracy in droop-controlled DC microgrids with both mesh and radial configurations*, Energies, vol. 8, no. 5, pp. 3591–3605 (2015).

[11] Xu Q. *et al.*, *A Decentralized Dynamic Power Sharing Strategy for Hybrid Energy Storage System in Autonomous DC Microgrid*, IEEE Transactions on Industrial Electronics, vol. 64, no. 7, pp. 5930–5941 (2017).

[12] Hoang K.D., Lee HH., *Accurate Power Sharing with Balanced Battery State of Charge in Distributed DC Microgrid*, IEEE Transactions on Industrial Electronics, in press (2018).

[13] Lu X., Sun K., Guerrero J.M., Vasquez J.C., Huang L., Teodorescu R., *SoC-based droop method for distributed energy storage in DC microgrid applications*, 2012 IEEE International Symposium on Industrial Electronics, Hangzhou, CHN, pp. 1640–1645 (2012).

[14] Yu X., She X., Ni X., Huang A.Q., *System Integration and Hierarchical Power Management Strategy for a Solid-State Transformer Interfaced Microgrid System*, IEEE Transactions on Power Electronics, vol. 29, no. 8, pp. 4414–4425 (2014).

[15] Ahmadi R., Paschedag D., Ferdowsi M., *Closed-loop input and output impedances of DC-DC switching converters operating in voltage and current mode control*, IECON 2010 – 36th Annual Conference on IEEE Industrial Electronics Society, Glendale, AZ, pp. 2311–2316 (2010).